Non-Orthogonal Frequency Division Multiple Access

Tongyang Xu and Izzat Darwazeh

Department of Electronic and Electrical Engineering, University College London, London, UK

Email: tongyang.xu.11@ucl.ac.uk, i.darwazeh@ucl.ac.uk

Abstract—This paper proposes a frequency-domain multiple user access scheme termed non-orthogonal frequency division multiple access (NoFDMA), which maintains the same data rate per user while allowing more users to access via non-orthogonal user overlapping in a given spectral band. User side signal processing follows existing standards with minor modifications. Receiver side operation can jointly process signals from all the users. Computational complexity is investigated for NoFDMA, which shows slightly increased operations than the typical orthogonal frequency division multiple access (OFDMA). Nevertheless, effective spectral efficiency of NoFDMA, considering both raw spectral efficiency and computational complexity, is higher than that of OFDMA. The scalability of the multiple access scheme is flexible via tuning the user overlapping ratio. Simulation reveals that the number of accessed users is doubled using the NoFDMA strategy when compared with the traditional OFDMA scheme over the same spectral resource utilization.

Index Terms—Multiple access, frequency-domain, non-orthogonal, IoT, waveform, OFDMA, SEFDM, NoFDMA, spectral efficiency, secure communication.

I. INTRODUCTION

With the fast development of internet of things (IoT), the number of connected devices is significantly increased. The existing orthogonal multiple access (OMA) and orthogonal waveform schemes may no longer be sufficient to support the massive connectivity. Therefore, non-orthogonal concept starts to become attractive in IoT waveform designs [1], [2], [3] and multiple access [4], [5]. Work in [4] summarized the non-orthogonal concept in power-domain non-orthogonal multiple access (NOMA), code-domain sparse code multiple access (SCMA) and other domain techniques. All the techniques can superimpose signals from multiple users to enhance the spectral efficiency. At the receiver, an advanced successive interference cancellation (SIC) detector is applied to remove the inter-user interference.

Considering the domain diversity, we propose a frequency-domain multiple access scheme termed non-orthogonal frequency division multiple access (NoFDMA), which was inspired by the non-orthogonal waveform concept in [3]. In NoFDMA, the OFDM signals generated from each user are received concurrently at a base station via non-orthogonal user overlapping in frequency-domain. Due to the frequency-domain non-orthogonal user signal packing, partial frequency resources are saved and reserved for extra users, which is the main advantage of NoFDMA. A simplified user packing scheme of NoFDMA is illustrated in Fig. 1, in which both OFDMA and NoFDMA occupy the same frequency spectral

band while NoFDMA can accept an extra user. It should be noted in the illustration that the bandwidth per sub-carrier is B_s for both multiple access systems indicating the same data rate per user. Therefore, NoFDMA is able to support higher total data rate than OFDMA. Robust signal detection is therefore required at the base station to mitigate inter-user interference. Deep learning based signal detector [6] has no domain-knowledge requirement but with limited interference cancellation performance. Sphere decoding (SD) detector [7] performs well in recovering signals from interference but is limited to small size systems (e.g. small number of sub-carriers and low order modulation formats) due to its sophisticated signal processing. Advanced techniques such as the multi-sphere architecture [8] can simplify signal detections to small block detections with performance promises. In this work, we focus on a realistic narrowband IoT (NB-IoT) [9] scenario, which follows LTE standard [10] but occupies 12 sub-carriers over 180 kHz bandwidth. Such a narrow bandwidth, equivalent to only a single physical resource block (PRB) in LTE, relieves frequency selective channel distortions [11]. In many applications, IoT devices are commonly static (no mobility) after deployment, which removes Doppler effects. Better yet, the maximum modulation scheme supported by NB-IoT is QPSK. All the specifications of NB-IoT pave the way for the straightforward realization of NoFDMA.

This work aims to inspire a new multiple access strategy in *frequency-domain*. The principle of NoFDMA is firstly introduced followed by a fair bit error rate (BER) performance comparison with orthogonal frequency division multiple access (OFDMA). Then the computational complexity and spectral efficiency of NoFDMA are analyzed with numerical comparisons. The proposed frequency-domain non-orthogonal multiple access strategy is applicable to traditional communication systems. In addition, it is able to support secure communications since signal detections for multiple users have to be operated jointly at the base station relying on the sophisticated SD [7] or the multi-sphere detectors [8].

II. PRINCIPLE OF NOFDMA

To illustrate, for a typical OFDMA system, represented by Fig. 2(a), we assume that three users are allocated total spectral resources of bandwidth B for access. Each user applies inverse fast Fourier transform (IFFT) to generate orthogonal frequency division multiplexing (OFDM) signals at data rate R_{user}. After the channel, the signals coming from
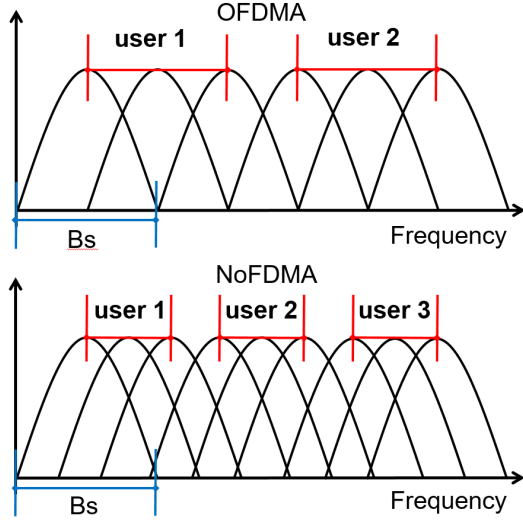
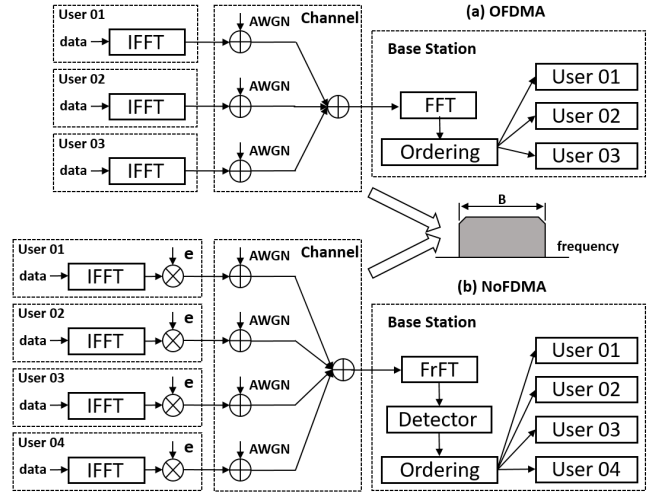Fig. 1. User packing (overlapping) scheme of NoFDMA. The bandwidth per sub-carrier is B_s.

Fig. 2. Principle of NoFDMA. In a given spectral bandwidth B, more users are aggregated in NoFDMA via non-orthogonally overlapping users.

three users are orthogonally aggregated at the receiver and processed jointly via a single fast Fourier transform (FFT) operation. Demodulated symbols are sorted and distributed to each user. For the proposed NoFDMA system in Fig. 2(b), also occupying the spectral bandwidth B, four users are allowed simultaneous access. Since the data rate per user maintains R_{user}, therefore higher spectral efficiency is achieved in NoFDMA. Generally, each user in NoFDMA applies IFFT to generate OFDM signals. However, an extra phase term, noted as e, is multiplied by the signal of each user. At the receiver, user signals are non-orthogonally added together with inter-user interference. Therefore, a fractional Fourier transform (FrFT) has to be used instead of FFT for signal demodulation. In addition, a signal detector is applied as well to mitigate the inter-user interference. Since signal detection work is within a base station, therefore the computational complexity at the receiver is not a big issue. Finally, an ordering module is used to sort and distribute symbols to corresponding users.

The NB-IoT specifications in [10] reserve options for new sub-carrier allocation and modulation schemes, which offer an opportunity for the NoFDMA development. The algorithm of user resource allocation in NoFDMA is described in Algorithm 1 and a specific example is presented in Table I, which demonstrates an extension from the 3-user (U_b=3) OFDMA scheme to 4,5,6-user (U_a=4,5,6) NoFDMA schemes.

In terms of the NoFDMA system, the continuous signal in each user is expressed as

$$x_i(t) = \frac{1}{T} \int_0^T s_i(l) \exp\left(\frac{j2\pi lrt}{T}\right) dt, \quad (1)$$

where i indicates the user index with the range $[0, 1, ..., U_a - 1]$, $s_i(l)$ is the N_a-dimension vector of the ith user consisting of sparsely allocated QPSK/BPSK symbols based on the resource allocation matrix $\mathbf{M}$ in Algorithm 1.

Algorithm 1 : NoFDMA user resource allocation scheme.

$U_b \in [1, 2, ..., 12]$; {No. of users in OFDMA}
$U_a \in [U_b, U_b + 1, ..., 24]$; {No. of users in NoFDMA}
$N_b = 12$; {No. of total sub-carriers in OFDMA}
$r = U_b/U_a \leq 1$; {User ratio}
$N_a = N_b/r$; {No. of total sub-carriers in NoFDMA}
$N_{per} = N_b/U_b$; {No. of sub-carriers per user in OFDMA and NoFDMA}
if $U_b < U_a < 2U_b$ **then**
    $modulation = BPSK, QPSK$;
else if $U_a = 2U_b$ **then**
    $modulation = BPSK$;
end if
for $\gamma = 0$; $\gamma \leq N_a U_b - 1$; $\gamma + +$ **do**
    if $mod(\gamma, U_b) == 0$ **then**
        $w(\gamma) = 1$; {'1' indicates the γth resource is allocated to a user}
    else
        $w(\gamma) = 0$; {'0' indicates the γth resource is not allocated to a user}
    end if
end for
$len = N_a U_a - N_a U_b$;
$P = [w, zeros(1, len)]$; {P is an $N_a U_a$ length vector}
for $\beta = 0$; $\beta \leq N_a - 1$; $\beta + +$ **do**
    $\mathbf{M}(\beta, :) = P(\beta U_a : \beta U_a + U_a - 1)$; {$\mathbf{M}$ is an $N_a \times U_a$ matrix}
end for

Table I: An example of NoFDMA user resource allocation.

N_{per}	U_b	N_b	U_a	N_a	Modulation
4	3	12	4	16	QPSK/BPSK
4	3	12	5	20	QPSK/BPSK
4	3	12	6	24	BPSK

Following the typical OFDM IFFT generation method, shown in Fig. 2(b), the discrete format of (1) is given as

$$X_i[k] = \frac{1}{\sqrt{N_a}} \sum_{l=0}^{N_a - 1} s_i(l) \exp\left(\frac{j2\pi lk}{N_a}\right), \quad (2)$$

where $X_i[k]$ is the kth modulated symbol from the ith user with $k = 0, 1, ..., N_a - 1$.

After the IFFT signal generation for each user, a complex exponential term, which is the phase rotation term e in Fig. 2

has to be multiplied in (2) giving a new expression as

$$\bar{X}_i[k] = \frac{1}{\sqrt{N_a}} \exp\left(\frac{j2\pi ik}{N_a U_a}\right) \sum_{l=0}^{N_a-1} s_i(l) \exp\left(\frac{j2\pi lk}{N_a}\right). \quad (3)$$

At the receiver, the signals from U_a users are superimposed leading to $Y[k]$, which is the received signal combining all the users as

$$Y[k] = \frac{1}{\sqrt{N_a}} \sum_{i=0}^{U_a-1} \exp\left(\frac{j2\pi ik}{N_a U_a}\right) \sum_{l=0}^{N_a-1} s_i(l) \exp\left(\frac{j2\pi lk}{N_a}\right)$$
$$+ \sum_{i=0}^{U_a-1} Z_i,$$

$$(4)$$

where Z_i is the additive white Gaussian noise (AWGN) of the ith user. The expression ignores frequency selective channel impairments due to the narrow bandwidth of each signal, which has been theoretically explained in [11]. Equation (4) can be further rearranged as

$$Y[k] = \frac{1}{\sqrt{N_a}} \sum_{i=0}^{U_a-1} \sum_{l=0}^{N_a-1} s'(i + lU_a) \exp\left(\frac{j2\pi(i + lU_a)k}{N_a U_a}\right)$$
$$+ \sum_{i=0}^{U_a-1} Z_i,$$

$$(5)$$

where $s'(i + lU_a) = s_i(l)$. By substituting with $n = i + lU_a$, (5) can be simplified to

$$Y[k] = \frac{1}{\sqrt{N_a}} \sum_{n=0}^{N_a U_a-1} s'(n) \exp\left(\frac{j2\pi nk}{N_a U_a}\right) + \sum_{i=0}^{U_a-1} Z_i. \quad (6)$$

Taking into account the user ratio r, (6) is converted to

$$Y[k] = \frac{1}{\sqrt{N_a}} \sum_{n=0}^{N_a-1} s(n) \exp\left(\frac{j2\pi nrk}{N_a}\right) + \sum_{i=0}^{U_a-1} Z_i, \quad (7)$$

where (7) is equivalent to the inverse fractional Fourier transform (IFrFT) operation and $s(n)$ is an N_a-dimension vector of symbols as

$$s(n/U_b) = s'(n), \ n \bmod U_b = 0, \ n = 0, 1, ..., N_a U_b - 1. \quad (8)$$

The recovered symbol vector $s(n)$ includes N_a QPSK/BPSK symbols from U_a users. The index of the N_a symbols is not consistent with the user index. The allocation principle of N_a symbols to U_a users follows the resource allocation matrix $\mathbf{M}$ in Algorithm 1.

There are different solutions of demodulating the signal in (7). The direct approach is to use matched filter (MF), which multiplies (7) with an exponential term $\exp(-j2\pi nrk/N_a)$. However, due to the fractional parameter r introduced in (1), inter-user interference between the mth sub-carrier in a user and the nth sub-carrier in a user is given as

$$u_{m,n} = \frac{1}{T} \int_0^T \exp\left(\frac{j2\pi mrt}{T}\right) \exp\left(\frac{j2\pi nrt}{T}\right)^* dt$$
$$= sinc[2\pi(m - n)r]$$
$$+ j \cdot \pi(m - n)r \cdot sinc^2[\pi(m - n)r]$$

$$(9)$$

$$\Re\{u_{m,n}\} = \begin{cases} Non-zero & 0.5 < r < 1, m \neq n \\ 0 & r = 0.5, m \neq n \end{cases}$$

$$(10)$$

$$\Im\{u_{m,n}\} = \begin{cases} Non-zero & 0.5 < r < 1, m \neq n \\ Non-zero & r = 0.5, m \neq n \end{cases}$$

$$(11)$$

Cross correlation, which yields inter-user interference when $m \neq n$, is studied for its real and imaginary parts in (10) and (11), respectively. It is observed that when $0.5 < r < 1$, both real and imaginary results are non-zeros indicating inter-user interference in both parts. However, when $r = 0.5$, the real part is '0' while its imaginary part is non-zero. This discovery reveals that for one-dimension modulation scheme such as BPSK, the inter-user interference can be avoided in its real part when $r = 0.5$. However, for $0.5 < r < 1$, both QPSK and BPSK will cause inter-user interference in real and imaginary parts, and robust signal detection has to be applied.

To remove efficiently the inter-user interference of non-orthogonal user signal superimposition at a base station, the SD detector [7], which can jointly decode signals from interference for all users, is employed.

III. MODELLING BER PERFORMANCE

The simulation is operated in a simple AWGN channel (not frequency selective) according to the channel frequency selective conditions in [11]. In addition, this work considers a stable communication scenario where IoT devices are static after their deployments. Therefore, Doppler effect is not taken into account. This work aims to inspire a new multiple access strategy in frequency-domain. Therefore, this section focuses on a fair comparison between NoFDMA and OFDMA. To have comparisons with other domain multiple access techniques (power-, code- space-), more efforts have to be made, which will be our future work.

The performance of each user in the 4-user (U_a=4) NoFDMA system is illustrated in Fig. 3(a), in which all the users show similar performance approaching the typical 3-user (U_b=3) OFDMA. The average performance of the 4-user NoFDMA, shown in Fig. 3(b), is similar to that of the 3-user OFDMA while occupying the same spectral bandwidth. With the increase of accessed users, the performance becomes worse as shown in Fig. 3(c)(d). Both the individual user performance and average user performance have approximately 2 dB power penalty when compared with the 3-user OFDMA. This indicates that higher inter-user interference is introduced with the increased number of simultaneously accessed users. To narrow the performance gap, new signal detection methods have to be developed, which is under investigation. For the 6-user (U_a=6) scenario shown in Fig.
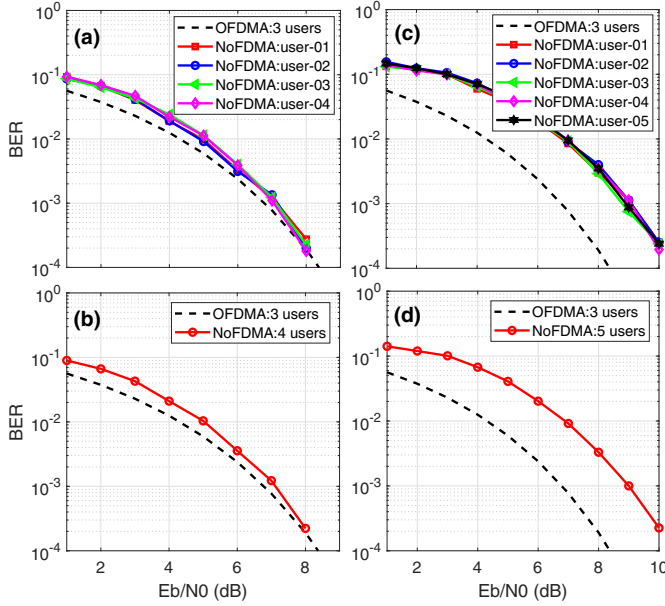
Fig. 3. Performance of NoFDMA when U_a=4 users are non-orthogonally accessed in (a)(b) and U_a=5 users are non-orthogonally accessed in (c)(d). The OFDMA with U_b=3 users has the same individual user performance and average user performance due to the orthogonal user overlapping. QPSK modulation is applied for all the scenarios.
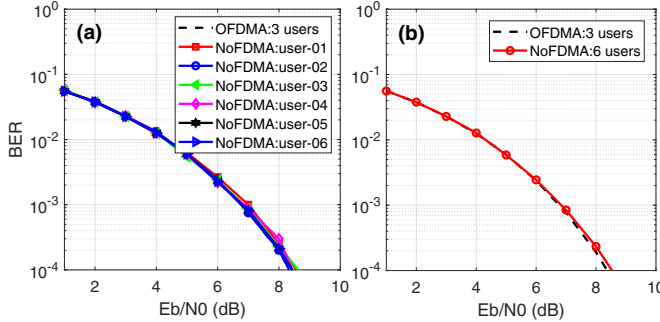

Fig. 4. Performance of NoFDMA when U_a=6 users are non-orthogonally accessed. BPSK modulation is applied for both scenarios.

4, due to the real part orthogonality, one-dimension BPSK modulation scheme enables the same performance for both OFDMA and NoFDMA.

IV. COMPUTATIONAL COMPLEXITY AND SPECTRAL EFFICIENCY

This work focuses on uplink IoT multiple access scenarios and the base station is responsible for receiver side signal processing. Since base stations are not sensitive to digital signal processing resource consumption, therefore the data rate and processing time delay of the NoFDMA technique maintain at the similar level when compared with OFDMA. In terms of complexity, the base station complexity is not taken into account and only IoT user side computational complexity

Table II: Per user complexity in terms of the number of complex operations for OFDMA and NoFDMA. The parameter N is the IFFT size.

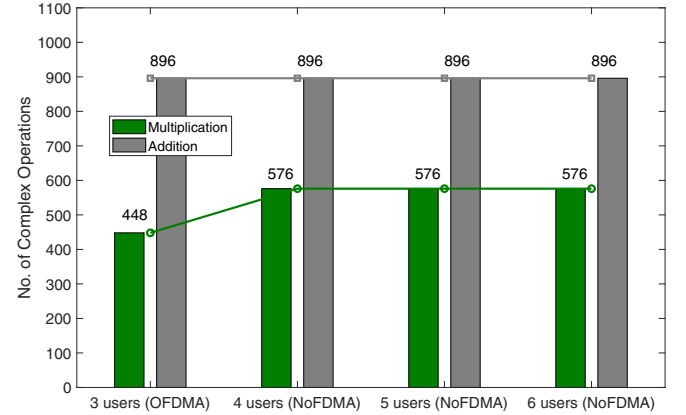| Operations	Multiplication	Addition
OFDMA	$\frac{N}{2} \times log_2 N$	$N \times log_2 N$
NoFDMA	$\frac{N}{2} \times log_2 N + N$	$N \times log_2 N$

Fig. 5. Per user complexity in terms of complex multiplication and addition in different multiple access scenarios.

is considered. Computational complexity, in the number of complex multiplication and addition operations per user, is presented in Table II. It should be noted that the complexity is mainly determined by the IFFT size and the minimum IFFT size set by the 3GPP NB-IoT standard [9], [10] is N=128. Therefore, both OFDMA and NoFDMA have to employ the same IFFT (N=128) for signal generation while NoFDMA requires extra N operations for the phase term multiplications shown in Fig. 2(b).

The numerical comparison of per user complexity is shown in a bar chart in Fig. 5. Scenarios with different number of accessed users ranging from three to six are compared. It is clearly seen that more additions are needed than multiplications for all user access cases. In addition, both OFDMA and NoFDMA require the same number of additions while NoFDMA requires extra multiplication operations because of the phase term multiplications in Fig. 2(b).

Raw spectral efficiency (SE) values are calculated following $log2(O)/r$ where O is the constellation cardinality (O=2 for BPSK and O=4 for QPSK). Fig. 6 presents the raw SE results in different number of users and modulation formats. QPSK modulation is not supported when the number of users is doubled. Therefore, the QPSK result for the NoFDMA with 6 users is not illustrated. It is clearly seen the improvement of SE from OFDMA to NoFDMA. However, these are raw SE results and complexity is not taken into account.

For a fair comparison, computational complexity should be included in the SE calculation leading to the effective SE in
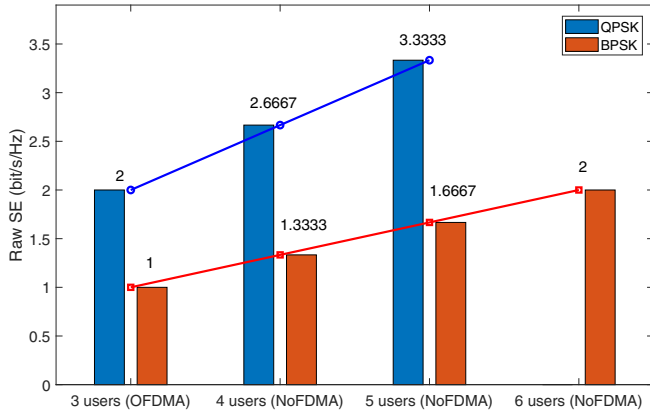
Fig. 6. Raw spectral efficiency for different multiple access scenarios with either BPSK or QPSK modulations.
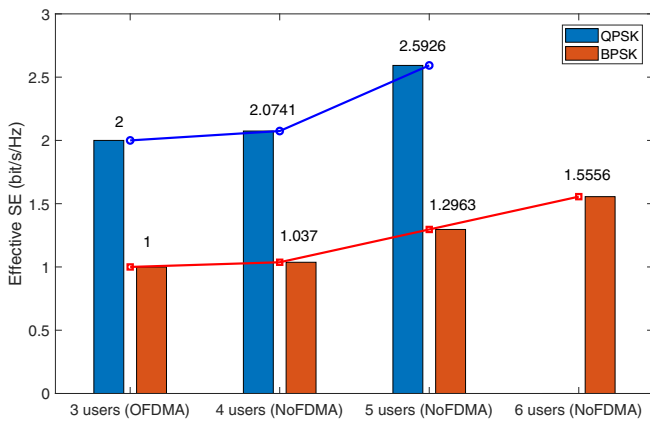

Fig. 7. Effective spectral efficiency for different multiple access scenarios with either BPSK or QPSK modulations.

Fig. 7, which jointly considers the raw SE in Fig. 6 and the computational complexity in Fig. 5. Due to the same addition operations for all the access schemes, only multiplications are counted here. To get a meaningful SE demonstration, normalized complexity is applied here which converts the number of multiplications in OFDMA to unit '1' and all other numbers in NoFDMA are scaled on the basis of the unit '1'. Therefore, the effective SE is computed as $SE_e = SE_{raw}/C_n$

where C_n is the normalized complexity in multiplications. The results in Fig. 7 show NoFDMA achieving better effective SE than OFDMA in all scenarios.

V. CONCLUSION

This work addresses user non-orthogonal multiple access in frequency-domain. Compared with OFDMA, the proposed NoFDMA, designed with a new user resource allocation scheme, maintains the same data rate per user (device) but supports more users to access the network without occupying extra spectral resources. We demonstrate an efficient signal generation method for users and an efficient joint signal decoding solution at the base station. Results show a much improved spectral efficiency of the new NoFDMA scheme by doubling the number of accessed users but at the expense of a slight increase in computational complexity.

REFERENCES

[1] S. Mahama, Y. J. Harbi, A. G. Burr, and D. Grace, "A non-orthogonal waveform design with iterative detection and decoding for narrowband IoT applications," in *2019 European Conference on Networks and Communications (EuCNC)*, Jun. 2019, pp. 315–319.

[2] L. Rugini and G. Baruffa, "BER of nonorthogonal FSK for IEEE 802.15.4," in *29th IEEE PIMRC*, Sep. 2018, pp. 570–571.

[3] T. Xu, C. Masouros, and I. Darwazeh, "Waveform and space precoding for next generation downlink narrowband IoT," *IEEE Internet of Things Journal*, vol. 6, no. 3, pp. 5097–5107, Jun. 2019.

[4] L. Dai, B. Wang, Y. Yuan, S. Han, C. I, and Z. Wang, "Non-orthogonal multiple access for 5G: solutions, challenges, opportunities, and future research trends," *IEEE Communications Magazine*, vol. 53, no. 9, pp. 74–81, Sep. 2015.

[5] Z. Ding, Y. Liu, J. Choi, Q. Sun, M. Elkashlan, C. I, and H. V. Poor, "Application of non-orthogonal multiple access in LTE and 5G networks," *IEEE Communications Magazine*, vol. 55, no. 2, pp. 185–191, Feb. 2017.

[6] T. Xu, T. Xu, and I. Darwazeh, "Deep learning for interference cancellation in non-orthogonal signal based optical communication systems," in *2018 Progress In Electromagnetics Research Symposium - Spring (PIERS)*, Aug. 2018 (invited), pp. 241–248.

[7] B. Hassibi and H. Vikalo, "On the sphere-decoding algorithm I. expected complexity," *IEEE Transactions on Signal Processing*, vol. 53, no. 8, pp. 2806–2818, Aug. 2005.

[8] T. Xu and I. Darwazeh, "Multi-Sphere decoding of block segmented SEFDM signals with large number of sub-carriers and high modulation order," in *2017 International Conference on Wireless Networks and Mobile Communications (WINCOM)*, Nov. 2017, pp. 1–6.

[9] R. Boisguene, S. Tseng, C. Huang, and P. Lin, "A survey on NB-IoT downlink scheduling: Issues and potential solutions," in *13th IEEE IWCMC*, Jun. 2017, pp. 547–551.

[10] 3GPP TS 36.213 v.14.2.0, "LTE; evolved universal terrestrial radio access (E-UTRA); physical layer procedures," Rel. 14, Apr. 2017.

[11] G. Ku and J. M. Walsh, "Resource allocation and link adaptation in LTE and LTE-Advanced: A tutorial," *IEEE Communications Surveys Tutorials*, vol. 17, no. 3, pp. 1605–1633, thirdquarter 2015.